Development of a global cloud resolving model
– a multi-scale structure of tropical convections –

Masaki Satoh[1, 2*], Hirofumi Tomita[1], Hiroaki Miura[1], Shinichi Iga[1] and Tomoe Nasuno[1]

[1] *Frontier Research Center for Global Change, Japan Agency for Marine-Earth Science and Technology*
[2] *Center for Climate System Research, University of Tokyo*

Abstract We have developed a global cloud resolving model, that is a new high resolution atmospheric general circulation model. It is a grid model with icosahedral structure and is based on the non-hydrostatic equations. The new model is called Nonhydrostatic ICosahedral Atmospheric Model (NICAM). At present, the first version of the model is almost completed. We evaluated the model performance by several test cases on the Earth Simulator, and found a very good computational efficiency.

The main target is high-resolution climate simulations by improving representation of cumulus convection with resolutions less than 5 km in horizontal directions. The global cloud resolving approach enables us to avoid use of cumulus parameterization that is one of the most ambiguous components of current climate modeling.

We have performed global cloud-resolving simulations with super-high resolutions on an aqua planet setup using NICAM. We studied the resolution dependency of the results and found that the simulations with grid intervals of 7 km and 3.5 km well capture hierarchical structure of clouds from cloud resolving scale to global scale. These successful results suggest that the global cloud-resolving simulation becomes one of promising approaches in the climate research field in the near future.

Keywords: nonhydrostatic model, cloud resolving model, cloud cluster, atmospheric general circulation model, aqua planet experiment

1. Introduction

A next generation high-resolution global atmospheric model that can calculate multi-scale structure from cumulus convection to the global circulation is being developed at Frontier Research Center for Global Change, Japan Agency for Marine-Earth Science and Technology. It is expected to run a 5 km or less horizontal resolution atmospheric model if the full performance of the Earth Simulator is achieved. At such a high resolution, it will be able to run more accurate numerical simulations of the global atmosphere without using cumulus parameterization, which is one of the most uncertain factors in the current climate models. At the same time, we need to switch to use the nonhydrostatic equations for the governing equations of the new model instead of the hydrostatic primitive equations that are the governing equations of the currently used global atmospheric models. Recently, global nonhydrostatic models are being developed at many institutes([1][2]; the Met Office [3]; and the

Canadian Meteorological [4]). Although the high-resolution model can be used for short term numerical predictions such as a week, we intend to use it as a climate model by integrating for sufficiently long days to obtain statistically equilibrated states of the atmosphere. To this end, we reconsider the structure of the new model from the basics instead of taking the former approach used for the existing general circulation models (GCMs). A unified model approach both to short term numerical prediction and to climate simulation is already taken by the Met Office (and the Hadley Centre's climate model) [3]. Our model is a unique nonhydrostatic model based on a quasi uniform grid, i.e. the icosahedral grid, which is very efficient on the Earth Simulator described below.

Our model development started since the year 2000. At the first stage, we take the following two paths of the development. The first is the investigation of new grid systems. It is pointed out that the performance of the usual spectral transform models and the latitude-longi-
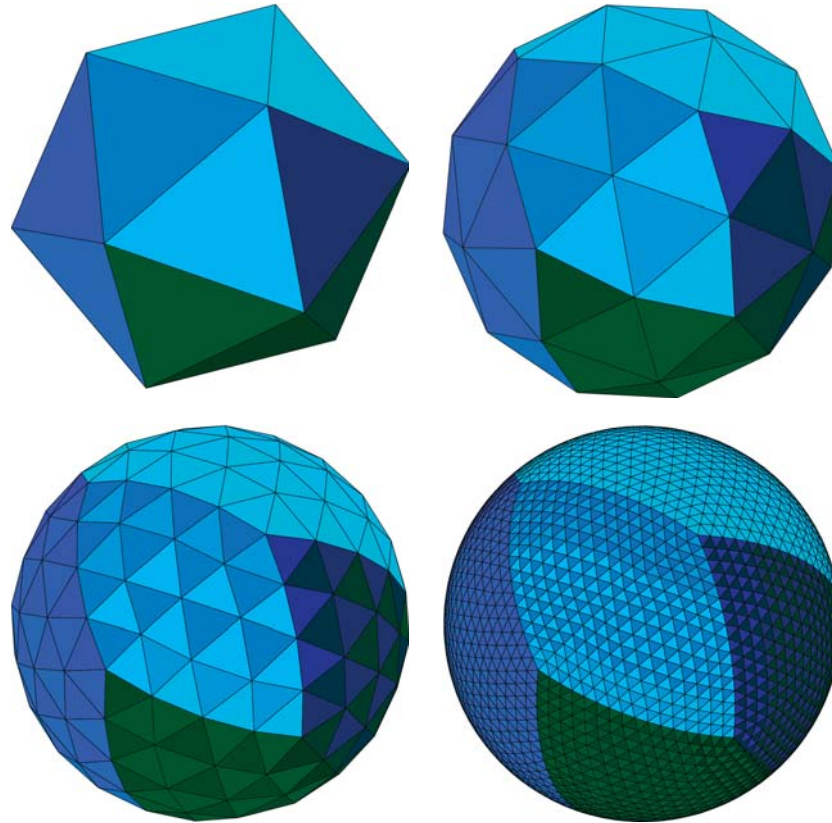
Fig. 1 The icosahedral grids. Grid division level (glevel) is 0 (left top), 1 (right top), 2 (left bottom), and 4 (right bottom).

tude grid models will be severely limited as resolution is increased. Through this preliminary investigation, we have decided to choose a quasi-uniform grid system represented as icosahedral grids depicted by Figure 1 as the grid system of our new atmospheric model. We examined the computational efficiency and accuracy by constructing a global shallow water model based on the icosahedral grid system [5] [6].

Second, we have newly developed a dynamical framework of the nonhydrostatic model. Although there are established nonhydrostatic models which are proved to be successful in short range numerical simulations as regional models or cumulus resolving models, there are a few used for long term integrations as climate simulation. In particular, most of the existing models do not guarantee conservation of mass and energy. Since our new nonhydrostatic model is aimed to be used for climate study, we have engaged in development a new dynamical scheme that can run for a long time duration with conserving mass and energy [7] [8].

The dynamical core of the newly developed global three-dimensional model was tested with several numerical experiments [9]. Then, the full physical global cloud resolving model is developed by installing physical processes, i.e., cloud microphysics, radiation, and boundary layer processes. This model is called Nonhydrostatic ICosahedral Atmospheric Model (NICAM).

The existing GCMs are used for horizontal resolution of about 100 km or up to a few tens of km, and the physical processes for GCMs are tuned to represent large-scale fields for such resolutions. In particular, cumulus parameterization is employed to represent statistical effects of cumulus convection. Since our new high-resolution model is aimed to be run at 5 km or less grid interval, we do not need to use cumulus parameterization based on statistical assumptions. We can explicitly resolve cumulus motions using cloud microphysical processes. Thus, our approach can treat explicitly the multi-scale and multi-physical interactions of clouds. Recently, the need for this approach for climate modeling is being advocated by Randall et al. [10].

In this paper, we describe outlines of the global nonhydrostatic modeling and show numerical results on the Earth Simulator in Section 2. In Section 3, as a first result from a global cloud resolving simulation, we show a numerical result of an aqua planet experiment. We conclude in Section 4 and list up further tasks.
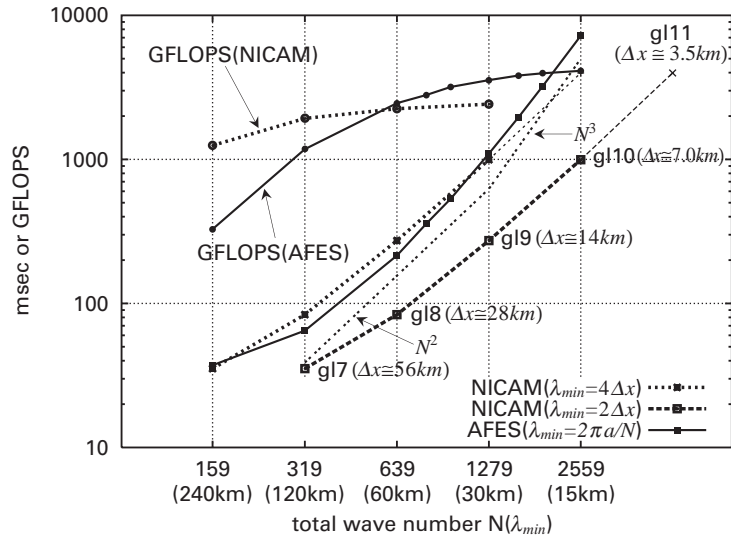
Fig. 2 Comparison of computational time for one time step between NICAM and AFES. The sustained performances are also shown.

2. Computer performance of the dynamical core

The *dynamical core* stands for governing equations of dynamics and their numerical discretization of a numerical model. The dynamical core is a central part of a numerical model and does not include physical processes such as radiation and clouds. Since results of climate models are sensitive to choices of complex physical processes, the numerical and computer performance of the dynamical core should be examined in various perspectives if one aims to develop a new model. In this section, we describe the computer performance of the dynamical core of NICAM.

NICAM is a nonhydrostatic global model using the icosahedral grids shown by Figure 1. The icosahedral grids are constructed by a recursive division of geodesic arches on the sphere. Starting from the original icosahedron, one-level finer grids are generated by bisecting the geodesic arches of the former coarser grids. We call the *n*-th bisection of the icosahedron *glevel n* (glevel: grid division level). The average grid interval of glevel 11 is about 3.5 km, for example. Numerical models with this grid system are first investigated by Sadourny et al. [11] and Williamson [12], and are recently revisited as a candidate for next-generation high-resolution global models [13] [14] [15]. We have made modifications to the original icosahedral grids by using the spring dynamics; with this modification, the fractal structure of the original icosahedral grid is relaxed and more uniform grid structure with a smaller ratio of minimum to maximum grid intervals is obtained by smoothing the grid arrangement. We found that the numerical errors are reduced using the modified grid [5] [6].

The governing equations of the global model are a newly developed nonhydrostatic schemes that guarantees conservation of mass and energy [7] [8] [9]. The finite volume method is used for the flux form equations. The Arakawa-A type grid is used where all the variables are allocated at the vertices of triangles. The shape of the control volume is either hexagon or pentagon. We evaluate the advection of momentum using three components of the three-dimensional Cartesian coordinates fixed to the space and do not need calculations of the metric terms for advection. We use the deep atmosphere equations where the effect of radius of the earth is counted and all the components of the Coriolis terms including vertical components are included; thus, the conservation of angular momentum is guaranteed in analytic form. Our icosahedral grids have wide flexibility; it can be further modified to any structure as long as the geometric relations between grid points are preserved. For instance, we can construct a stretched grid by concentrating grids at some locations in Asia with coarsening resolutions in the other hemisphere. This stretched grid model can be used as a regional climate model.

Figure 2 compares the computational time on the Earth Simulator required for one time step integration of a dynamical core experiment. These data are measured with a standard experiment proposed by Held and Suarez [16], widely used for evaluation of dynamical cores of GCMs. The same experiment is performed both with NICAM and AFES (AGCM for the Earth Simulator), which is an Eulerian spectral transform atmospheric GCM well tuned for the Earth Simulator [17] [18]. We

Table 1 Comparison of maximum time step and computational time required for one day simulation of Held and Suarez experiment between NICAM and AFES, when 80 nodes of the Earth Simulator are used. The value for glevel 11 is an estimated time.

NICAM	glevel 7	glevel 8	glevel 9	glevel 10	glevel 11
Δx	56 km	28 km	14 km	7 km	3.5 km
Δt [sec]	450.00	225.00	112.50	56.250	28.125
1 day time [sec]	6.72	32.26	209.66	1519.10	(12159)
AFES	T159	T319	T639	T1279	T2559
Δt [sec]	400.00	200.00	100.00	50.000	25.000
1 day time [sec]	7.99	28.80	184.32	1883.52	24928.13

use 80 nodes where each node has 8 processors; the corresponding peak performance is 5TFlops. The abscissa is the total wave number N of the triangular truncation or the horizontal resolution λ_{min}. Some remarks are required before giving interpretation of this figure, since there is ambiguity in determining resolution of numerical models [19] [20]. In general, the horizontal resolution of the spectral model is given by $\lambda_{min} = 2\pi a/N$, where a is the radius of the earth. For the grid model, we may have $\lambda_{min} = 2\Delta x$ since the shortest wave is represented by two grid points. In the case of the Arakawa-A grid (the co-allocated grid) as we do, however, it might be difficult to give physical meanings to the shortest wave with $2\Delta x$. Thus, one might say that the resolvable scale is $\lambda_{min} = 4\Delta x$ for the A-type grid. Figure 2 shows that while the curve for AFES approaches asymptotically to the line N^3, the curve for NICAM approaches the line N^2 as resolution becomes higher. If we interpret the resolution of NICAM as $\lambda_{min} = 2\Delta x$, this shows that NICAM is almost one-order magnitude efficient in comparison to AFES for all the resolutions. If the resolution of NICAM is interpreted as $\lambda_{min} = 4\Delta x$, the efficiency of NICAM becomes superior to AFES at higher resolutions than T1279. It must be noted that this data should be observed as a tentative since the computational efficiency can be further tuned. Each model has its advantages other than computational efficiency, so that comparison between different models must be made from various perspectives.

Table 1 shows a maximum time step for each of the resolutions and the CPU time required for one day simulation. The columns of this table are aligned so as to relate the resolutions $\lambda_{min} = 4\Delta x$ of NICAM to those of $\lambda_{min} = 2\pi a/N$ of AFES. The time steps of both models Δt are constrained by the CFL condition for the advection and they are almost similar values at the corresponding resolutions, though a slightly longer time step can be taken for NICAM. This table also indicates that the time required for one day simulation is shorter for NICAM than AFES at least higher resolutions than glevel 10 or T1279. As remarked above, there remains the interpretation of model resolution in order to compare models with different structures.

3. Global cloud resolving calculations

As a first global cloud resolving simulation with NICAM, we have performed an aqua planet experiment using the Earth Simulator. An aqua planet experiment is an idealized numerical experiment on the earth-like planet, on which the surface is assumed to be ocean everywhere. It is a suitable experimental setup for studying behavior of cloud convection in the tropics. Recently, Neale and Hoskins [21] propose a series of aqua planet experimental setup as international intercomparison experiments. We use the surface temperature distribution of the control experiment proposed by Neale and Hoskins [21], and specify the ozone distribution and the equinoctial solar incident with diurnal cycle.

By implementing physical processes to NICAM, we have developed a global cloud resolving model. We use the cloud microphysics scheme proposed by Grabowski [22], which is a simple two-category scheme suitable for climate study with the ice effects considered. The two-stream adding method for the radiation [23], the Meller-Yamada level-2 closure scheme for the turbulence, and the bulk method by Louis et al. [24] for the surface flux scheme are used.

We first integrate a coarser resolution model with grid interval of 14 km (glevel 9) for 60 days as a spinup run, and then run the model with grid interval of 7 km (glevel 10) for 30 days (the 7 km-run). Using the result at day 20 obtained with the 7 km-run as the initial condition, we integrate the model with grid interval of 3.5 km (glevel 11) for 10 days (the 3.5 km-run). In the vertical direction, 54 levels are used with stretched intervals. We use the same physical schemes for these three experiments regardless of the resolution. Comparison between three runs is discussed in [25]. We show the results from the 7 km-run and the 3.5 km-run in this paper from the viewpoint of the precipitation rate.

Figure 3 shows the global distribution of precipitation averaged for 1.5 hours at day 85 of the 3.5 km-run. This shows a multi-scale structure of cumulus convection in
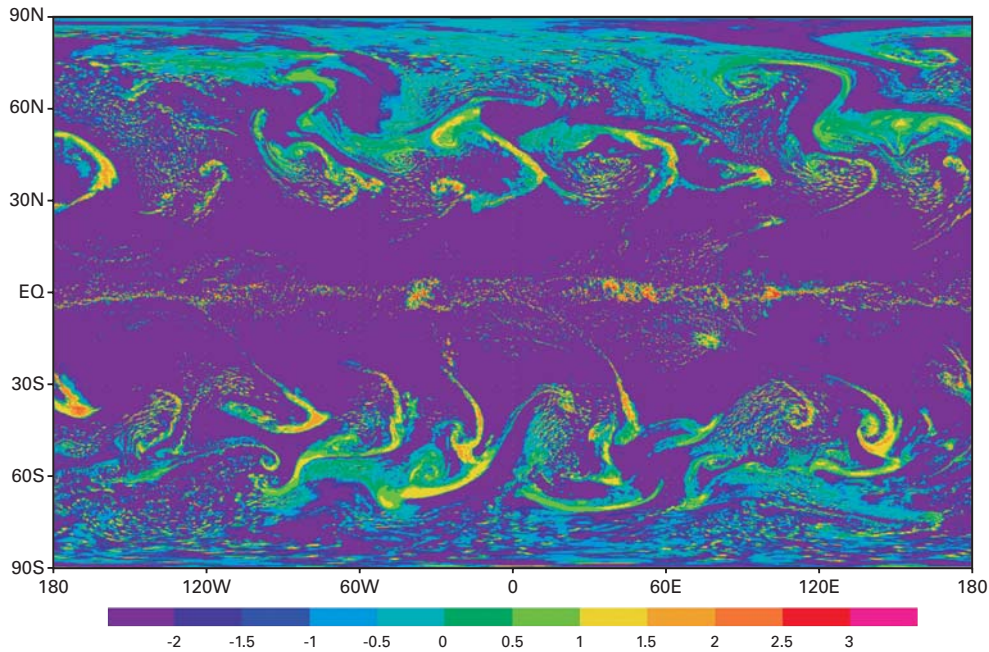
Fig. 3 Global distribution of precipitation for 1.5 hours average at day 85 of the 3.5 km-run. The color scale is log_{10} (precipitation rate [mm day^{-1}]).
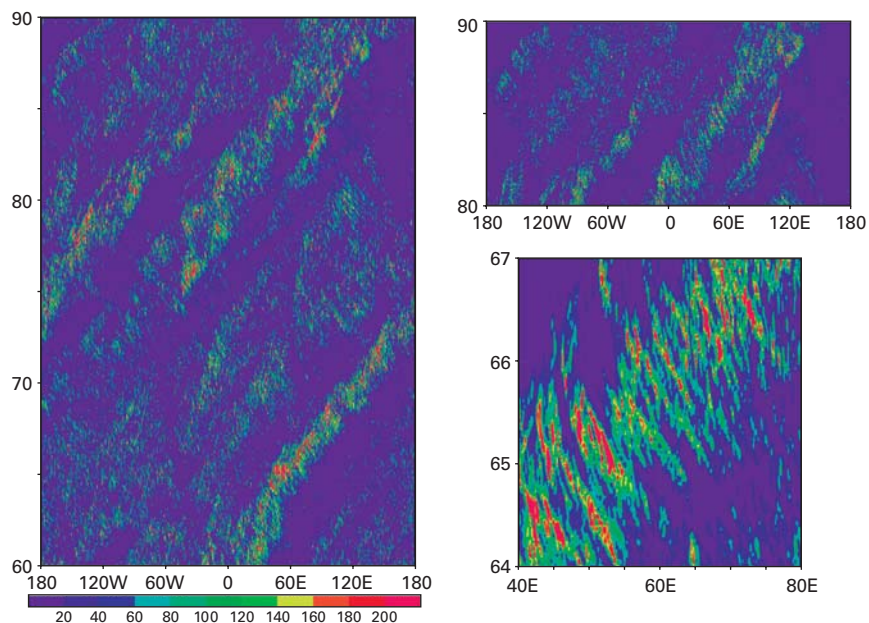

Fig. 4 Hovmöller diagrams of precipitation along the equator averaged in latitudes 2°N-2°S. (left) 7 km-run, (right top) 3.5 km-run, and (right bottom) zoomed up for 7 km-run in the region days 64-67 and latitudes 40E-80E. Unit is mm day^{-1}.

the tropics: there is a precipitation belt along the equator, i.e. the intertropical convergence zone (ITCZ). The ITCZ has an organized structure in longitudinal direction, the intensive cloud areas with horizontal scale of 4000-5000 km are thought to be super cloud clusters: the largest super cloud cluster is centered at around 50°E, and smaller super cloud clusters are located at around 100°E and 40°W. The super cloud clusters consist of cloud clusters with horizontal scale of 100-200 km. For example, several cloud clusters are aligned along the equator in 30-60°E. Within the cloud clusters, furthermore, we can see intensive precipitation with size of a few kilometers, which corresponds to individual cumulus convections.

Figure 4 is the Hovmöller diagrams of precipitation of the 7 km-run and the 3.5 km-run. These show temporal variation of longitudinal distribution of precipitation
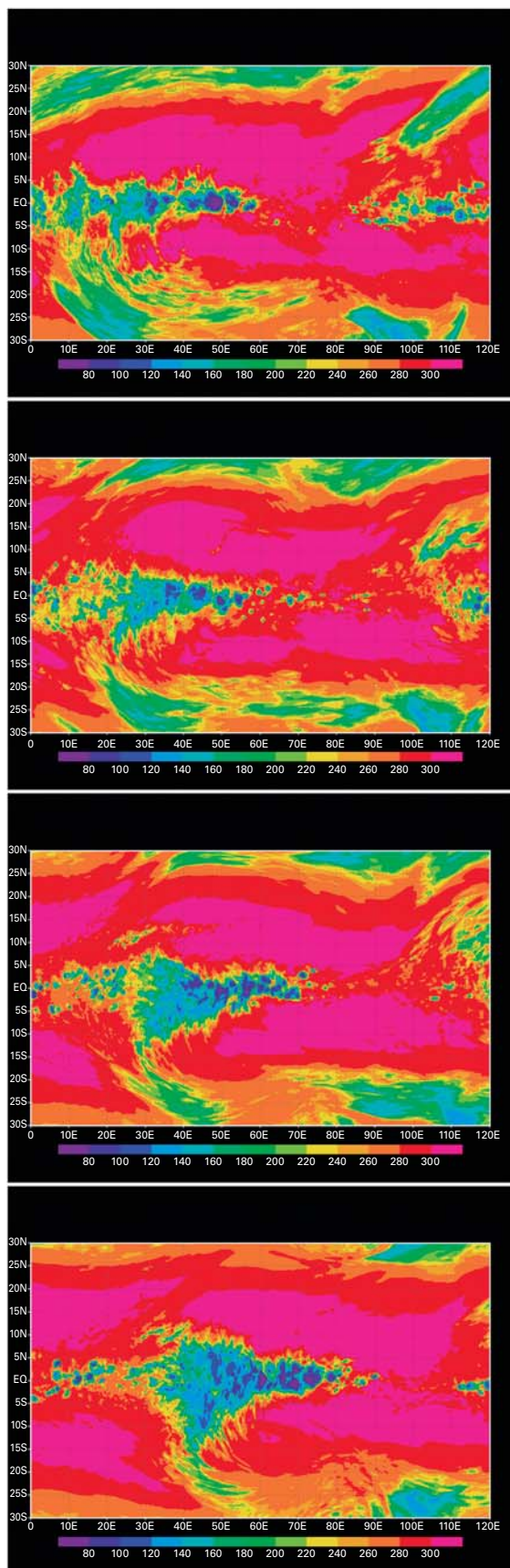
Fig. 5 The outgoing longwave radiation (OLR) of the 7 km-run showing eastward propagation of the super cloud cluster. From the top, at days 62, 63, 64, and 65 averaged over three hours between 15-18 h. Unit is W m^{-2}.
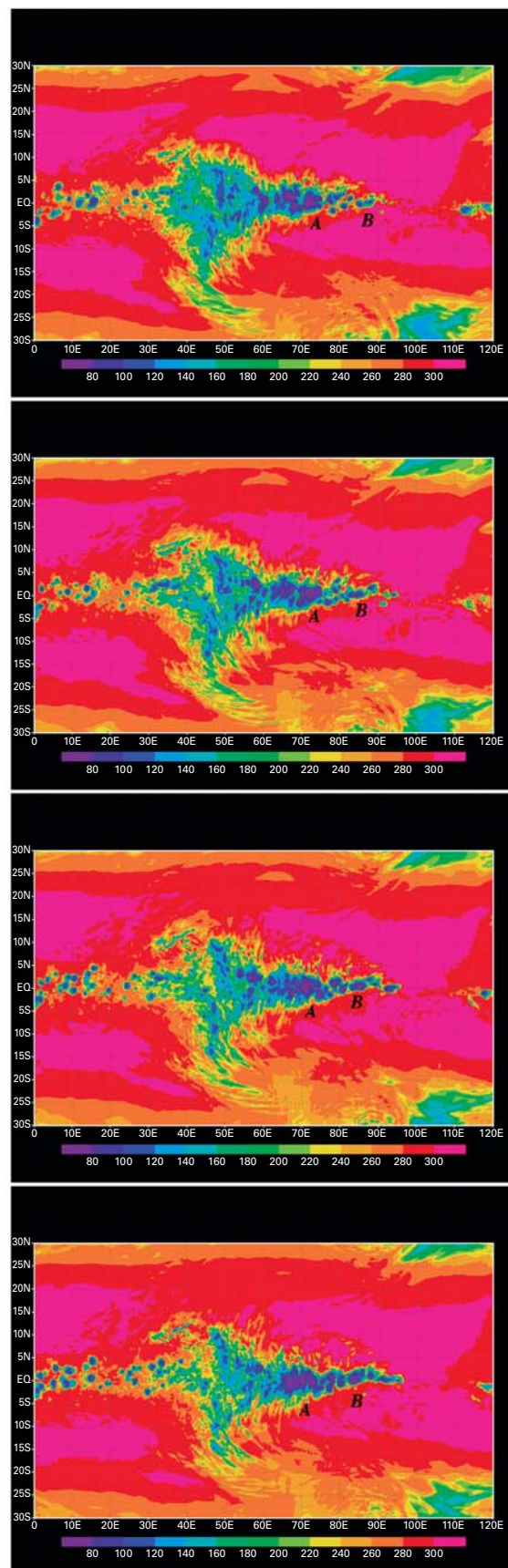
Fig. 6 The outgoing longwave radiation (OLR) of the 7 km-run showing westward movement of the cloud clusters. From the top, at day 65, 18-21 h; day 65, 21-24 h; day 66, 0-3 h; and day 66, 3-6h averaged over 3 hours. Unit is W m^{-2}.

Table 2 Computational performance of the aqua planet experiments with NICAM.

NICAM	glevel 9	glevel 10	glevel 11
Δx	14 km	7 km	3.5 km
Δt [sec]	30	30	15
nodes	80	320	320
1 day time [hr]	0.64	0.81	5.28
GFLOPS	1911.8	7607.6	7701.5
sustained performance[%]	37.3	37.1	37.6

along the equator averaged over latitudes between 2°N-2°S. In both runs, eastward propagation of large-scale organized structure is clearly emerged. This propagation of precipitation pattern is similar to the observed convectively-coupled Kelvin wave associated with the intraseasonal variation or the Madden-Julian oscillation (MJO) [26] [27]. The wave number one is most prominent, and the distributions of surface pressure and zonal winds are similar to those of the Kelvin wave [25]. The propagation speed of the super cloud clusters in the 7 km-run and the 3.5 km-run is slower than that in the 14 km-run, and is closer to the observation: about 25-30 days to travel around the equator. The eastward propagation of the super cloud clusters is an envelope of westward motions of each of cloud clusters with size of 100-200 km (right bottom panel of Fig. 4). The phase speed of the westward motions of cloud cluster is about 10 m s⁻¹, which is about one third of the westward propagation speed of the super cloud clusters.

A sequence of the eastward propagation of the super cloud cluster is shown in 4 panels of Figure 5; These are the outgoing longwave radiation (OLR) of 3 hours average over 15-18 h at days between 62 and 65. The eastern end of this super cloud cluster is about 60°E at day 62, while it reaches about 90°E at day 65. The shape of the super cloud cluster is changing; it elongates along the equator at day 62, but becomes a triangle with its western end being the base; the eastern end is concentrated near the equator, and the western end spreads out to 15° in both hemispheres, to which the cold front of the mid-latitude extratropical cyclones is connected. Details of the super cloud cluster are shown in Figure 6 with a three hours interval. Each cloud cluster moves westward (as denoted by A and B), while the super cloud cluster as an envelope of the cloud clusters propagate eastward. At the eastern end of the super cloud cluster, a new cloud cluster is generated as denoted by B.

These figures reveal the multi-scale structure in the tropics: intensive precipitation as a scale of cumulus, i.e., a few km, cloud clusters as a scale of hundreds of km, and super cloud clusters as a scale of several thousands of km. The largest scale is the wave number one associated

with an equatorial Kelvin wave like structure. These calculations can only be realized by using the global cloud resolving model on the Earth Simulator.

The computer performance of the aqua planet experiment is summarized in Table 2. Since the physical processes are included, one-day simulation times are longer than those shown in Table 1. At the 3.5 km-run, we take the time step $\Delta t = 15$ s, which is shorter than that shown in Table 1; we use this relatively shorter time step in order to avoid accidental abortion of the run. If $\Delta t = 30$ s can be used for the 3.5 km-run, about 2.5 hours are required to run one-day simulation for a global cloud resolving model.

4. Summary and further plans

We have developed the global cloud resolving model called NICAM at Frontier Research Center for Global Change. The dynamical core of this model is based on the nonhydrostatic equations and the icosahedral grid structure. The numerical scheme of this model guarantees conservation of mass and energy by using the finite volume method. Especially in high resolutions less than 10 km, the computational efficiency on the Earth Simulator shows that NICAM is superior to AFES, which is a dedicated spectral model well tuned for the Earth Simulator.

As a first global cloud resolving simulation, we have performed an aqua planet experiment by implementing various physical processes such as cloud microphysics to NICAM. A multi-scale structure from the cloud scale precipitation to the global scale structure of the convectively-coupled Kelvin wave is simultaneously calculated. Both the westward moving cloud clusters and the eastward propagating super cloud clusters coexist in the model simulation. The detailed structure of the convectively-coupled Kelvin wave is analyzed in [25]; in which the propagation of clouds is shown in the field of the outgoing longwave radiation, while this paper analyzed that of the precipitation rate.

The present result is only for the aqua planet setup in order to isolate the behavior of clouds on the open ocean condition. Preliminary results show that the diurnal cycle of the precipitation of an aqua planet resembles with that

observed on an open ocean [25]; the diurnal cycle is compared with that of the similar aqua planet experiment using a parameterized convection [28]. Of course there are some limitation to the results associated with the configuration of the model in terms of a global aqua-planet, and one should be careful in the interpretation of their results. We are about to run a global cloud resolving experiment under a more realistic condition with a land-sea distribution.

Comparison between the simulation results of global cloud resolving experiments and the satellite analysis such as the Tropical Rainfall Measurement Mission (TRMM) data will reveal characteristics of clouds in the tropics. This global cloud resolving approach will lead to improvement of climate predictions and seasonal weather forecasts by simulating multi-scale structure ranging from cloud scale to the global scale and multi-physics such as cloud and radiation processes. Shorter range and seasonal weather predictions will be improved by more accurate representations of cloud activities in the tropics, such as diurnal cycles of convections, generation of tropical cyclones, and the intraseasonal variations. As longer range predictions, climate simulations will be more reliable through improvements of cloud properties in the tropics and statistics of hydrological cycles including distributions of water vapor.

Acknowledgment

(This article is reviewed by Dr. Julia Slingo.)

References

[1] F. H. M. Semazzi, J. H. Qian and J. S. Scroggs, A global nonhydrostatic semi-Lagrangian atmospheric model without orography, *Mon. Wea. Rev.*, vol.**123**, pp.2534–2550, 1995.

[2] J.-H. Qian, F. H. M. Semazzi and J. S. Scroggs, A global nonhydrostatic semi-Lagrangian atmospheric model with orography, *Mon. Wea. Rev.*, vol.**126**, pp.747–771, 1998.

[3] M. J. P. Cullen, T. Davies, M. H. Mawson, J. A. James, S. C. Coutler and A. Malcolm, An overview of numerical methods for the next generation U.K.NWP and climate model, Numerical methods in Atmospheric and Oceanic Modelling, The Andrew J. Robert Memorial Volume, C.A. Lin et al. Eds., NRC Research Press, pp.425–444, 1997.

[4] K.-S. Yeh, J. Cote, S. Gravel, A. Methot, A. Patoine, M. Roch and A. Staniforth, The CMC-MRB global environmental multiscale (GEM) model. Part III: Nonhydrostatic formulation, *Mon. Wea. Rev.*, vol.**130**, pp.329–356, 2002.

[5] H. Tomita, M. Tsugawa, M. Satoh and K. Goto, Shallow water model on a modified icosahedral geodesic grid by using spring dynamics, *J. Comput. Phys.*, vol.**174**, pp.579–613, 2001.

[6] H. Tomita, M. Satoh and K. Goto, An optimization of the icosahedral grid modified by the spring dynamics, *J. Comput. Phys.*, vol.**183**, pp.307–331, 2002.

[7] M. Satoh, Conservative scheme for the compressible nonhydrostatic model with horizontally explicit and vertically implicit time integration scheme, *Mon. Wea. Rev.*, vol.**130**, pp.1227–1245, 2002.

[8] M. Satoh, Conservative scheme for a compressible nonhydrostatic models with moist processes, *Mon. Wea. Rev.*, vol.**131**, pp.1033–1050, 2003.

[9] H. Tomita and M. Satoh, A new dynamical framework of nonhydrostatic global model using the icosahedral grid, *Fluid Dyn. Res.*, vol.**34**, pp.357–400, 2004.

[10] D. A. Randall, M. Khairoutdinov, A. Arakawa and W. W. Grabowski, Breaking the cloud-parameterization deadlock, *Bull. Amer. Meteor. Soc.*, vol.**84**, pp.1547–1564, 2003.

[11] R. Sadourny, A. Arakawa and Y. Mintz, Integration of the nondivergent barotropic vorticity equation with an icosahedral-hexagonal grid for the sphere, *Mon. Wea. Rev.*, vol.**96**, pp.351–356, 1968.

[12] D. L. Williamson, Integration of the barotropic vorticity equation on a spherical geodesic grid, *Tellus*, vol.**20**, pp.642–653, 1968.

[13] G. R. Stuhne and W. R. Peltier, New icosahedral gridpoint discretizations of the shallow water equations on the sphere, *J. Comput. Phys.*, vol.**148**, pp.23–58, 1999.

[14] R. Heikes and D. A. Randall, Numerical integration of the shallow-water equations on a twisted icosahedral grid. Part I: Basic design and results of tests, *Mon. Wea. Rev.*, vol.**123**, pp.1862–1880, 1995.

[15] D. Majewski, D. Liermann, P. Prohl, B. Ritter, M. Buchhold, T. Hanisch, G. Paul, W. Wergen and J. R. Baumgardner, The operational global icosahedral-hexagon gridpoint model GME: Description and high-resolution tests, *Mon. Wea. Rev.*, vol.**130**, pp.319–338, 2002.

[16] I. M. Held and M. J. Suarez, A proposal for the intercomparison of the dynamical cores of atmospheric general circulation models, *Bull. Am. Meteorol. Soc.*, vol.**75**, pp.1825–1830, 1994.

[17] S. Shingu, H. Takahara, H. Fuchigami, M. Yamada, Y. Tsuda, W. Ohfuchi, Y. Sasaki, K. Kobayashi, T. Hagiwara, S. Habata, M. Yokokawa, H. Itoh and K. Otsuka, A 26.58 Tflops global atmospheric simulation with the spectral transform method on the Earth Simulator, In Proceedings of the 2002 ACM/IEEE SC2002

Conference. ACM, 2002. http://www.sc-2002.org/paper-pdfs/pap.pap331.pdf.

[18] W. Ohfuchi, H. Nakamura, M.K. Yoshioka, T. Enomoto, K. Takaya, X. Peng, S. Yamane, T. Nishimura, Y. Kurihara and K. Ninomiya, 10-km mesh meso-scale resolving simulations of the global atmosphere on the Earth Simulator – Preliminary outcomes of AFES (AGCM for the Earth Simulator). *J. Earth Sim.*, vol.**1**, pp.8–34, 2004.

[19] R. Laprise, The resolution of global spectral models, *Bull. Amer. Meteor. Soc.*, vol.**73**, pp.1453–1454, 1992.

[20] R.A. Pielke, A recommended specific definition of "resolution", *Bull. Amer. Meteor. Soc.*, vol.**72**, p.1914, 1991.

[21] R. B. Neale and B. J. Hoskins, A standard test for AGCMs including their physical parametrizations: I:The proposal, *Atmospheric Science Letter*, vol.**1**, doi:10.1006/asle.2000.0019, 2001.

[22] W. W. Grabowski, Toward cloud resolving modeling of large-scale tropical circulation: A simple cloud microphysics parameterization, *J. Atmos. Sci.*, vol.**55**, pp.3283–3298, 1998.

[23] T. Nakajima, M. Tsukamoto, Y. Tsushima, A. Numaguti and T. Kimura, Modeling of the radiative process in an atmospheric general circulation model, *Applied Optics*, vol.**39**, pp.4869–4878, 2000.

[24] J. F. Louis, M. Tiedke and J.-F. Geleyn, A short history of the PBL parameterization at ECMWF, Workshop on Planetary Boundary layer Parameterization, ECMWF, Reading, U.K., pp.59–80, 1982.

[25] H. Tomita, H. Miura, S. Iga, T. Nasuno and M. Satoh, A global cloud-resolving simulation: Preliminary results from an aqua planet experiment, *Geophys. Res. Lett.*, vol.**32**, L08805, doi:10.1029/2005GL022459, 2005.

[26] T. Nakazawa, Tropical super clusters within intraseasonal variations over the western pacific, *J. Meteor. Soc. Japan*, vol.**66**, pp.823–839, 1988.

[27] Y. N. Takayabu, T. Iguchi, M. Kachi, A. Shibata and H. Kanzawa, Abrupt termination of the 1997-98 El Niño in response to a Madden-Julian oscillation, *Nature*, vol.**402**, pp.279–282, 1999.

[28] S. J. Woolnough, J. M. Slingo and B. J. Hoskins, The diurnal cycle of convection and atmospheric tides in an aqua-planet GCM, *J. Atmos. Sci.*, vol.**61**, pp.2559–2573, 2004.